



XA04N0666

VISUALIZATION OF VELOCITY FIELD AND PHASE DISTRIBUTION IN GAS-LIQUID TWO-PHASE FLOW BY NMR IMAGING

G.Matsui, H.Monji and J.Obata

Institute of Engineering Mechanics
University of Tsukuba, Tsukuba 305, Japan
FAX:(81)298-53-5207

ABSTRACT

NMR imaging has been applied in the field of fluid mechanics, mainly single phase flow, to visualize the instantaneous flow velocity field. In the present study, NMR imaging was used to visualize simultaneously both the instantaneous phase structure and velocity field of gas-liquid two-phase flow. Two methods of NMR imaging were applied. One is useful to visualize both the one component of liquid velocity and the phase distribution. This method was applied to horizontal two-phase flow and a bubble rising in stagnant oil. It was successful in obtaining some pictures of velocity field and phase distribution on the cross section of the pipe. The other is used to visualize a two-dimensional velocity field. This method was applied to a bubble rising in a stagnant water. The velocity field was visualized after and before the passage of a bubble at the measuring cross section. Furthermore, the distribution of liquid velocity was obtained.

INTRODUCTION

Detail information of flow velocity, turbulence, and phase distributions is important to understand a two-phase flow mechanism. To obtain information about the flow, there are two types of flow measurement: local (or point) and spatial. A laser Doppler anemometer, a hot-wires anemometer and a resistivity needle probes system belong to the former and a flow meter and an impedance ring meter of void fraction belong to the latter. The local measurement gives a detail structure of the flow but multi-point measurement is needed to obtain the spatial information. On the other hand, the spatial measurement gives the average value on a cross section, but does not give a detail structure. However, both spatial and local information is needed to understand a flow structure. Furthermore, a measurement method not to disturb flow is desirable. Imaging or visualization methods have been developed to satisfy such requirements. Recent development of visualization method can give information about an instantaneous and local flow structure on the measuring section without disturbance. In the study of two-phase flow, the visualization of phase structure using X-ray,¹ γ -ray,^{2,3} neutron⁴⁻⁸ and ultrasonic wave^{9,10} has been developed.

NMR (nuclear magnetic resonance) imaging is one of the such methods but may have some advantages. Recently, it has been possible to visualize not only the phase structure but

also the velocity field by use of NMR imaging. For example, NMR imaging was applied to the liquid single phase flow and the velocity field was clearly obtained in the transition region from laminar to turbulent flow.¹¹

In the present study, two methods of NMR imaging was used. One is a phase method with flow-sensitive magnetic field gradient.¹¹ The other is an imaging method with a spatial tagging sequence.¹²⁻¹⁶ The former method can simultaneously and instantaneously visualize both a phase structure and a one-component field of liquid velocity.¹⁷ The latter can visualize the two-dimensional velocity field of liquid.

EXPERIMENTAL EQUIPMENT

Two kinds of experimental equipment were used. One was a loop with a horizontal test section as shown in Fig.1. The inner diameter of the test section was 20mm. Water containing CuSO_4 crystals (0.25wt%) was circulated in the loop by a pump. The flow rate of the water was controlled by valves and measured by a turbine flow meter. A nitrogen gas was supplied to the mixer through a pressure gauge and a flow meter. The nitrogen gas was injected into the water at the mixer. A horizontal test section locates downstream of 1.8m from the mixer. The two-phase flow was observed just before the test section.

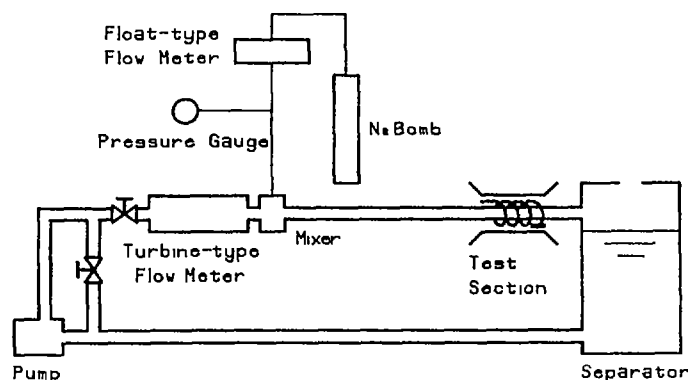


Fig.1 Schematic diagram of experimental apparatus for horizontal flow.

Table 1. Measuring conditions of NMR Imagings.

	Phase method		Imaging with a partial tagging sequence
	Horizontal flow	Rising bubble	
Time interval taking a image	200 ms		
Total data acquisition time	20.48 ms		40.96 ms
Image matrix	32 × 32		64 × 64
Dimension of visualized data area	24 mm × 24 mm		22.4 mm × 22.4 mm
Pixel dimension	0.75 mm	0.375 mm	0.35 mm
Thickness of slice plane	4 mm		

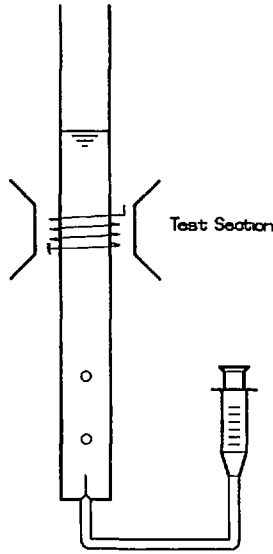


Fig.2 Schematic diagram of experimental apparatus for rising bubbles.

The other one was a simple vertical pipe (I.D. 18mm) as shown in Fig.2. A single bubble was generated by a needle injector (I.D. 0.47 mm) that was located on the bottom of the pipe. The gas was air and the liquid was water or oil (density 910kg/m³ and viscosity 53–60dyn/cm at 20°C). The generated bubble rose up slowly in the stagnant liquid. The test section was located 30 cm downstream of the bubble injection point.

INSTRUMENTATION

The NMR imaging system used a 1T iron-cored electromagnet for a static magnetic field. The diameter of the pole pieces and the gap between them were 300mm and 66mm, respectively. Three pairs of magnetic-field gradient coils were fixed to the magnet pole pieces. A solenoid coil with a diameter of 28mm and a length of about 30mm was used as both the transmitter and receiver coil. The measuring conditions of NMR imagings are shown in Table 1.

Phase Method

Before starting measurement, the static magnetic field is applied by the 1T iron-cored electromagnet. When a linear magnetic field gradient is applied, the precession frequency (Larmor frequency) of the nuclear spin is proportional

to the intensity of the gradient magnetic field. Therefore, the positions of the nuclear spins correspond to their precession frequencies, respectively. Thus, when the spins move along the magnetic field gradient, the precession frequency gradually changes. The resultant change of the frequency is observed as a phase shift of the nuclear spins' Larmor precession. Because this phase shift is proportional to the velocity component along the magnetic field gradient, the spins' velocity is obtained by the measurement of the phase shift. When a nuclear spin has instantaneous velocity components u , v and w at the position (y, z) on the measuring plane, the phase shift $\phi(y, z)$ is expressed as

$$\phi(y, z) = \alpha u(y, z) + \beta v(y, z) + \gamma w(y, z) \quad (1)$$

where α , β and γ are constants determined by the pulse sequence. Because these constants may be taken any values by designing the gradient waveforms, any velocity component can be obtained at the measurement. The phase shift $\phi(y, z)$, which is known from NMR imaging, contains three components of the velocity. It is necessary to take three images, in order to determine all the three components of the velocity. When the only one component of the velocity is needed or the instantaneous velocity field is needed, the one component can be obtained by setting two of α , β and γ on zero.

Two kinds of NMR images are obtained through the image reconstruction process. They are called real and imaginary images and their intensities $R(y, z)$ and $I(y, z)$ are expressed as

$$R(y, z) = k\rho(y, z) \cos \phi(y, z) \quad (2)$$

$$I(y, z) = k\rho(y, z) \sin \phi(y, z) \quad (3)$$

where k is a constant and $\rho(y, z)$ is the nuclear spin density on the measuring plane. Because the phase shift is proportional to the selected velocity component, the velocity distribution is visualized through the nonlinear function. In the present study, the nuclear spin of hydrogen was used. Because the hydrogen density in liquid is larger than that in the air, the phase structure can be measured by using the nuclear spin density $[\rho(y, z)]$ image.

$$\rho(y, z) = \sqrt{R(y, z)^2 + I(y, z)^2}/k \quad (4)$$

$$\begin{aligned} \phi(y, z) &= \tan^{-1} I(y, z)/R(y, z) \\ &= \alpha u(y, z) + \beta v(y, z) + \gamma w(y, z) \end{aligned} \quad (5)$$

Imaging with a Spatial Tagging Sequence

Figure 3 shows the initial grid pattern on the cross section of the pipe. The grid pattern is the density image represented by Eq.(4). The spatial grid is made by the magnetic pulse sequence pattern. In Fig.3, the nuclear spins on white square parts have precession by both the gradient and the static magnetic fields. There are the nuclear spins without precession on the black grid part.

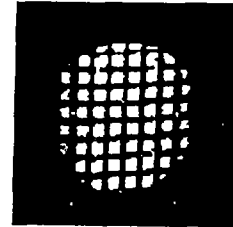


Fig.3 The initial grid pattern of NMR imaging with a spatial tagging sequence.

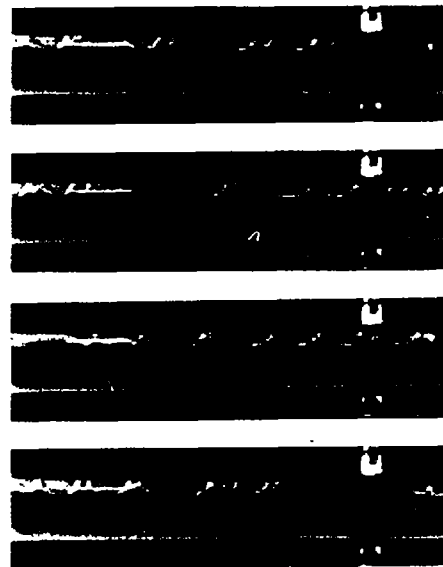
After making the grid on the measuring plane, the density image is taken. The grid pattern changes with the movement of the nucleus, which move with the flow. As the result, the associated white square parts change to the rhombus-like shapes. In the present study, the each shift of the face centers of the squares is detected. The face centers of the squares and the rhombus-like shapes are pointed on the two intensity images. The distance between two face centers of the square and the corresponding rhombus-like shape is calculated. The velocity of the face center is calculated from the distance and the time difference theoretically. However, in the study, the velocity is calibrated based on the calibration experiment result because the time difference between two images is not accurately known.

EXPERIMENTAL RESULTS

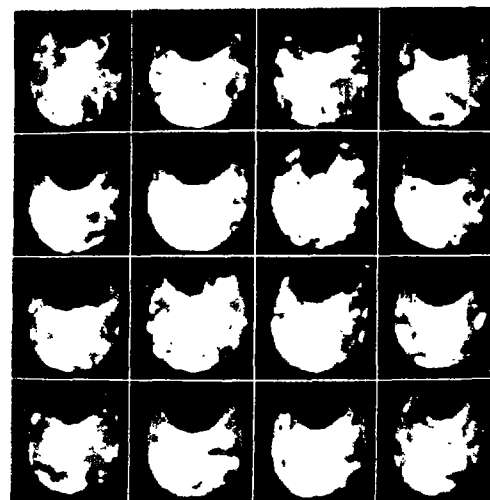
Phase Method

Figure 4-(a) shows pictures of the horizontal flow ($j_L=0.15\text{m/s}$, $j_G=0.016\text{m/s}$ and $\langle\alpha\rangle=0.096$) upstream of the test section. They were taken at every one second and time passes from the upper to the lower picture. The bubbles flowed continuously at the upper part of the pipe. Figure 4-(b) shows the nuclear spin density images on the cross section of the pipe. The images were taken at every 200ms and are displayed from the upper left to the lower right. The white part in the cross section shows the high density part of the nuclear spin or the liquid phase and the black part shows the low density or the gas phase. The nuclear spin density images show the phase structure in which bubbles located at the upper part of the pipe and the size of bubble changed with time. Figure 5-(a) shows the flow ($j_L=0.15\text{m/s}$, $j_G=0.08\text{m/s}$ and $\langle\alpha\rangle=0.35$) that had high gas flow rate and high liquid velocity, comparing with the flow shown in Fig.4. The flow pattern was slug flow and the gas-slugs flowed intermittently at the upper part of the pipe. Figure 5-(b) shows the nuclear spin density images displayed as the same way as in Fig.4-(b). The nuclear spin density images show the intermittent flow. The area and the shape of gas phase change with time, from left to right, and show the cross section of the gas-slug. The white images show the cross section of the liquid-slug.

The rising bubbles in the stagnant oil were measured by NMR imaging. The spherical bubble generated by the needle on the bottom plate was rising straight in the stagnant oil. The large bubble gives clear NMR images. Figure 6-(a) show the nuclear spin density $[\rho(y,z)]$ image on the left and the phase shift $[\phi(y,z)]$ image on the right. The circular cross section of the pipe is not displayed as a circle shown in Fig.6-(b) due to the video printer system. The black part at a white cross section of the pipe in the nuclear spin density image is the cross section of the bubble. The diameter of the bubble is about 7mm in the measuring plane and the rising velocity is about 12–18cm/s. At the location corresponding to the bubble in the phase shift image, there are a black or gray part and a white part. The brightness corresponds to the phase shift or the velocity (see

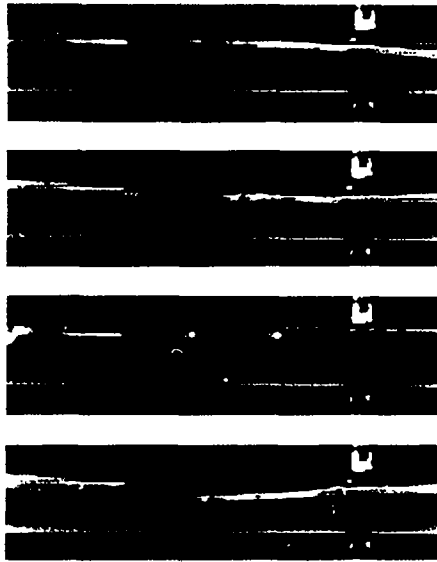


(a)Bubble flow.

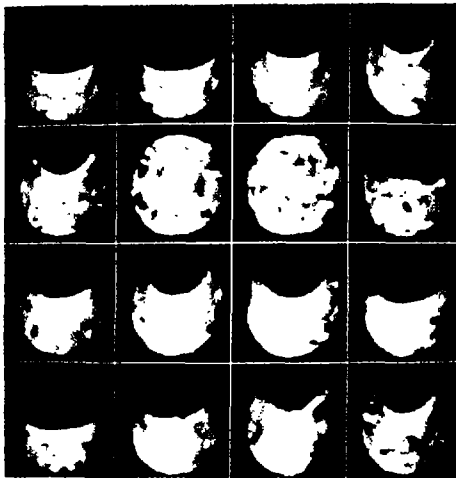


(b) The nuclear spin density images on the cross section for the horizontal flow.

Fig.4 NMR structure measurement of horizontal flow. $j_L=0.15\text{m/s}$, $j_G=0.016\text{m/s}$ and $\langle\alpha\rangle=0.096$.



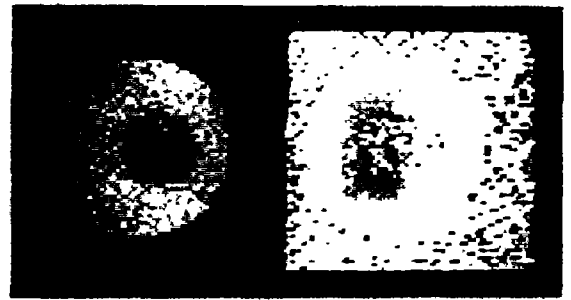
(a) Slug flow.



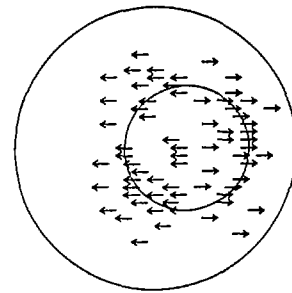
(b) The nuclear spin density images for the slug flow. Time passes from the upper left to the lower right. The images were taken at every 200ms.

Fig.5 NMR structure measurement of horizontal slug flow. $j_L=0.15\text{m/s}$, $j_G=0.08\text{m/s}$ and $\langle\alpha\rangle=0.35$.

Eq.(5)). Here, the visualized velocity is along the horizontal direction (perpendicular to the pipe axis) in Fig.6-(a). The white part has a velocity from the left to the right. The direction of the velocity in the black part is opposite to that of the velocity in the white part, as shown in Fig.6-(b) that is the illustration of the velocity field. When a bubble rises up in the liquid, the liquid flows down along the surface of the bubble. Then the liquid has the velocity component that is perpendicular to the bubble velocity. In the velocity field shown in Fig.6-(b), there is a counter flow around the bubble, that showed a front flow of the bubble.



(a) NMR images of the bubble. The left image shows the nuclear spin density and the right image shows the phase shift.



(b) Illustration of the velocity field.

Fig.6 NMR structure measurement of an air bubble rising a stagnant oil.

Imaging with a Spatial Tagging Sequence

Figure 7 shows the intensity images on the cross section of the pipe. These images were taken at every 200ms and time passes from the picture number 1 to 16. The picture 1 shows the image for the stagnant water. The picture 2 shows the cross sectional image for water and a bubble corresponding to the wane. The following images (3-15) show the movement of the water, after the bubble passed the measuring plane. Finally, the water became stagnant again as shown in the picture 16.

Figure 8-(a) shows the images from 0.8 s to 1.4 s later after the passage of the bubble at the measuring plane. The velocity fields are obtained based on these images. Because the water moved rapidly just after the bubble passed the measuring plane, the white square part was severely transformed or vanished away. Therefore, the velocity field was not able to be measured. Figure 8-(b) shows the velocity fields corresponding to Fig.8-(a). The directions of the arrows show those of the shifts of the white squares. Those are corresponding to the flow directions of the liquid. The lengths of the arrows show magnitude of the velocities. From these distributions, it is shown as follows. At 0.8 s later, it is observed that water flows toward the upper left part on the cross section corresponding to the location where the bubble passed through, as shown in Fig.8-(b). After that, the flow becomes weak with time. It is imagined that water flows to fill the volume of bubble, after the passage of the bubble.

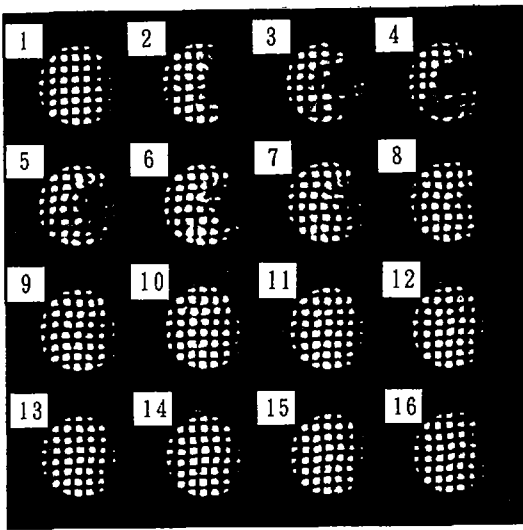


Fig.7 The time series images with a spatial tagging sequence. Time passes from 1 to 16. The time interval is 200 ms.

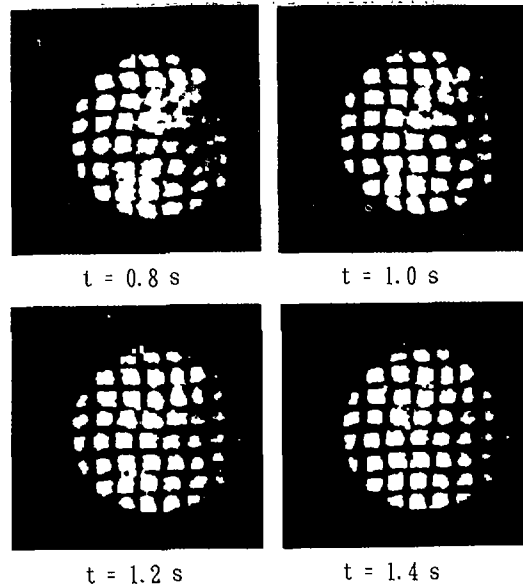
CONCLUSIONS

The NMR imaging has been applied to the gas-liquid two-phase flow, in order to visualize the instantaneous flow structure (both the phase structure and velocity field). Two different methods were used.

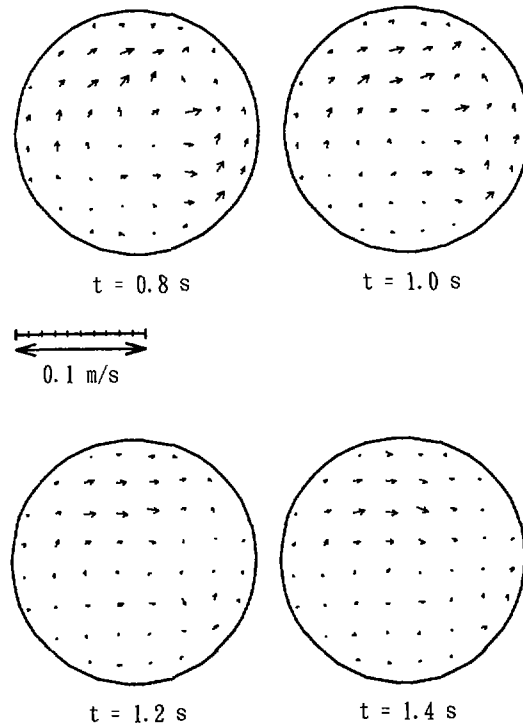
One is the phase method with flow-sensitive magnetic field gradient. The velocity field was visualized by using the phase shift of moving nuclear spins. The phase shift corresponds to the velocity of the nuclear spin contained in the liquid. The phase distribution was visualized by using the density of the nuclear spins, because the nuclear spin density of the gas-phase is different from that of the liquid-phase. In the experiment, the horizontal two-phase flow and the bubble rising in stagnant oil were measured. The nuclear spin density images showed the phase structure on the cross section for bubble or slow slug flow in the horizontal pipe. The location and the size of the rising bubble were measured by the nuclear spin density image. The one component of velocity field around the bubble was visualized by the phase shift image. The velocity field and the phase distribution were visualized simultaneously.

The other is the imaging with a spatial tagging sequence. This method can visualize the complex fluid motion in the single phase flow and is suitable for instantaneous visualization of a two velocity components field. Thus, this method was applied to the fluid motion around the rising bubble in the stagnant water to obtain the two velocity components field.

These experimental results show that the phase distribution and the liquid velocity field can be visualized and, therefore, that NMR imaging is useful for the structure measurement of two-phase flow.



(a) The images from 0.8 s to 1.4 s later after the passage of the bubble at the measuring plane.



(b) The velocity fields corresponding to the time series images (a).

Fig.8 The time series images and the velocity fields after the passage of the bubbles.

ACKNOWLEDGMENT

The authors thank Professor K.Kose, Institute of Applied Physics, University of Tsukuba, for use of NMR imaging system and helpful suggestions.

REFERENCES

1. N.HIRATA, T.NARABAYASHI, H.ISHIZUKA and T.KAGAWA, "Void Fraction Distribution Measurement by X-ray Beam through Image Reconstruction Technique and Analytical Simulation for Liquid Film Behavior", *Proc. Japan-U.S. Seminar on Two-Phase Flow Dynamics*, Lake Placid, B-4(1984).
2. A.M.C.CHAN, "A Single-Beam Multi-Detector Gamma Densitometer for Void Fraction and Phase Distribution Measurements in Transient Two-Phase Flows, *Measuring Techniques in Gas-Liquid Two-Phase Flows* (Springer-Verag), 281(1984).
3. R.T.LAHEY Jr. and K. OHKAWA, "An Experimental Investigation of Phase Distribution in an Eccentric Annulus", *Int. J. Multiphase Flow* 15, 447(1989).
4. A.H.ROBINSON and S.L. WANG, "High Speed Motion Neutron Radiography of Two-Phase Flow", *Neutron Radiography*, 653(1983).
5. D.H.C.HARRIS and W.A.J.SEYMOUR, "Applications of Real Time Neutron Radiography at Harwell", *Neutron Radiography*, 595(1983).
6. M.TAMAKI, K.OHKUBO, Y.IKEDA and G.MATSUMOTO, "Analysis of Two-Phase Counter Flow in Heat Pipe by Neutron Radiography", *Neutron Radiography*, 609(1986).
7. K.MISHIMA, S.FUJINE, K.YONEDA, K.YONEAYASHI, K.KANDA and H. NISHIHARA, "A Study of Air-Water Flow in a Narrow Rectangular Duct using an Image Processing Technique", *Proc. Japan-U.S. Seminar on Two-Phase Flow Dynamics*, (1988).
8. N.TAKENAKA, T.FUJII, A.Ono, K.SONODA, S.TAZAWA and T.NAKANII, "Application of Real-Time Neutron Radiography to Multiphase Flow Visualization and Measurement", *Proc. 3rd World Conference on Neutron Radiography*, (1989).
9. R.S.MACKAY and G.RUBISSOW Jr., "Decompression Studies Using Ultrasonic Imaging of Bubbles", *IEEE Trans. on Biomedical Eng. BME-25-6*, 537(1978).
10. J.S.CHANG, Y.ICHIKAWA and G.A.IRONS, "Flow Regime Characterization and Liquid Film Thickness Measurement in Horizontal Gas-Liquid Flow by an Ultrasonic Method", *Measurements in Polyphase Flows* 1982, 7(1982).
11. K.KOSE, "Visualization of Local Shearing Motion in Turbulent Fluids using Echo-Planar Imaging", *J. Magn. Reson.* 96, 596(1992).
12. E.A.ZERHPUNI, D.M.PARISH, W.J.ROSERS, A.YANG and E.P.SHAPIRO, *Radiology* 169, 59(1988).
13. L.AXEL and L.DOUGHERTY, *Radiology* 171, 841(1989).
14. L.AXEL and L.DOUGHERTY, *Radiology* 172, 349(1989).
15. T.J.MOSHER and M.B.SMITH, *Magn. Reson. Med.* 15, 334(1990).
16. K.Kose, "Visualization of Turbulent Motion Using Echo-Planar Imaging with a Spatial Tagging Sequence", *J. Magn. Reson.* 98, 599(1992).
17. G.MATSUI and H.MONJI, "Structure Measurement of Two-phase Flow Using NMR Imaging", *Proc. Japan-U.S. Seminar of Two-Phase Flow Dynamics*, Berkeley, 501(1992).